Polymer Chemistry

PAPER

View Article Online
View Journal | View Issue

Cite this: *Polym. Chem.*, 2014, **5**, 2253

Highly birefringent side-chain LC polymethacrylate with a dinaphthyl-acetylene mesogenic unit†

Sungmin Kang,* Shunpei Nakajima, Yuki Arakawa, Masatoshi Tokita, Junji Watanabe and Gen-ichi Konishi*

Received 31st October 2013
Accepted 8th December 2013

DOI: 10.1039/c3py01528a

www.rsc.org/polymers

We synthesised a highly birefringent liquid crystalline (LC) side-chain polymer based on polymethacrylate with a dinaphthyl-acetylene mesogenic unit in the side chain. Three polymer types with different carbon numbers in the terminal alkoxy chain (m = 1, 3 and 6) were prepared, and their optical properties as well as phase sequential behaviours were investigated. All polymers formed a nematic phase with a wide temperature range, and a smectic C phase was detected between the nematic and crystal phases when m was extended to 6. Notably, for homologous m = 1, we successfully obtained a nematic glassy-state LC film with high optical performance under ambient temperature conditions. The optical properties of this LC film were shown to be consistent with those of a highly birefringent, low molar mass LC material, with birefringence, extraordinary and ordinary refractive indices of 0.36, 1.82 and 1.46, respectively at 550 nm.

Introduction

Liquid crystals (LCs) have been widely used for manufacturing flat panel displays such as those used in televisions, personal computers and mobile phones. This, in turn, is leading to increasing use of high-birefringence (Δn) LCs for fabricating telecommunication devices,[1] laser emission films,[2] organic light-emitting diodes (OLEDs),[3] optical fibres[4] and photostorage devices.[5] The use of high-Δn LC materials in such applications is advantageous in not only reducing the size of the devices, *i.e.*, reducing cell gaps and film thickness, but also for reducing the cost of materials. It is known that to obtain the high-Δn property, introduction of a π-conjugation moiety along the molecular long axis is practical. To extend the conjugation length further, multiple bonds or unsaturated rings are commonly employed.[6–8] In our previous studies, dinaphthyl diacetylene (DNDA) and dinaphthyl acetylene (DNA) moieties were employed as mesogenic units. Consequently, the so-called DNDA-OCm and DNA-OCm (m is the carbon number of the tail) exhibit a wide temperature range corresponding to the nematic (N) LC regime and high Δn properties, reaching as high as 0.62 for DNDA-OC2.[9] Thus, the potential of DNDA and DNA derivatives as high-Δn LC materials for use in various optical applications was confirmed.

For use in such optical applications, it is also important for the developed materials to exhibit high-Δn properties at ambient temperatures. In this sense, a glassy film with uni-aligned LC polymers is a good candidate in terms of both optical properties and usage under ambient conditions, because it can provide high transparency by retaining a uniaxially aligned N orientation through vitrification. Recently, we reported the synthesis of highly birefringent polymethacrylates (PMs) with dialkoxy diphenyl-diacetylene (DPDA) moieties in the side chain.[10] The obtained polymer had a wider N phase regime than the monomer and it was successfully vitrified holding the N orientation. Further, the polymer exhibited a high birefringence with the highest value of 0.3 (at 550 nm) obtained at room temperature. However, to develop such polymers for practical use in optical devices, it is necessary to overcome the following problems: (1) monomer synthesis is difficult and asymmetric DPDA is prepared *via* reactions involving several steps, such as Sonogashira, Negishi and Corey–Fuchs reactions.[11,12] Therefore, the total monomer yield is relatively low. (2) Radical polymerisation cannot proceed in the presence of diaryl-diacetylene moieties; consequently, only an anionic polymerisation can be performed, which may not be practical.[13] (3) The obtained Δn value, 0.3, is high but still requires improvement through changes in the molecular design. As an effective strategy for overcoming these problems, we designed a PM with a highly birefringent DNA pendant group in the side chain.

In this study, we synthesised a high-Δn LC PM with a side chain mesogen based on DNA (Scheme 1) and succeeded in obtaining a N glassy film with high birefringence at room temperature. As mentioned above, the DNA moiety is a good candidate for generating a high-Δn material and offers the advantage of not trapping radicals during radical polymerisation. This synthesis was then successfully performed by free radical polymerisation, which allowed us to prepare three polymer types with differing alkoxy tail lengths. The phase

Department of Organic and Polymeric Materials, Tokyo Institute of Technology, Ookayama, Meguro-ku, Tokyo 152-8552, Japan. E-mail: skang@polymer.titech.ac.jp; konishi.g.aa@m.titech.ac.jp; Fax: +81-3-5734-2888; Tel: +81-3-5734-3641

† Electronic supplementary information (ESI) available: Synthetic procedures and NMR analysis data. See DOI: 10.1039/c3py01528a

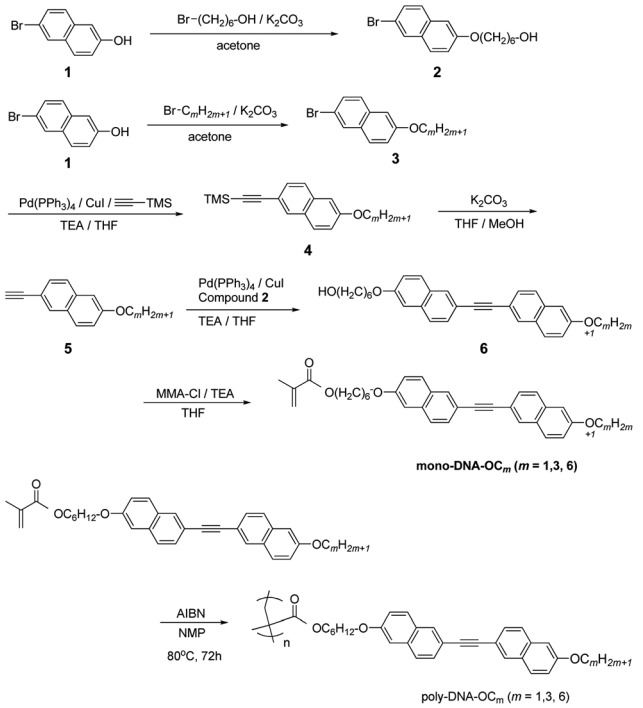

Scheme 1

transitional behaviours and optical properties, such as the ordinary and extraordinary refractive indices and birefringence, were examined.

Results and discussion

Synthesis

The synthetic route for side-chain LC type of PM with DNA-OC*m* (poly-DNA-OC*m*) is shown in Scheme 1. These novel monomers were mainly synthesised according to the following steps: (1) Williamson ether reaction for compound **1** and 6-bromo-1-hexanol; (2) Sonogashira coupling reaction for compound **3** and subsequent removal of a protecting trimethyl silyl group for compound **4** to obtain compound **5**; (3) Sonogashira coupling reaction for compound **5** and **2** (4) esterification between compound **6** and methacrylate chloride to obtain the monomers.[14] The monomers could be easily polymerised by employing conventional free radical polymerisation with azobisisobutyronitrile (AIBN). The polymers were soluble in organic solvents such as tetrahydrofuran and *N*-methylpyrrolidinone among others. The chemical structure of the monomers was confirmed by ^{1}H nuclear magnetic resonance (NMR) and ^{13}C NMR spectroscopy, and that of the polymers was confirmed by ^{1}H NMR spectroscopy.[15] The number average molecular weight, M_n and polydispersity of the polymers, M_w/M_n, were determined by gel permeation chromatography, which are listed in Table 1.

Table 1 Number average molecular weight (M_n) and polydispersity (M_w/M_n) for poly-DNA-OC*m*

m	1	3	6
M_n	30 000	27 000	56 000
M_w/M_n	1.91	1.98	2.18

Table 2 Phase transition behaviours of monomers and polymers[a]

Compound	Transition temperature/°C (enthalpy/kJ mol^{-1})
Mono-DNA-OC1	Cr 103.5 (37.1) N 159.0 (0.52) Iso
Mono-DNA-OC3	Cr 102.0 (20.7) N 183.2 (0.19) Iso
Mono-DNA-OC6	Cr 104.5 (5.57) N 157.0 (0.90) Iso
Poly-DNA-OC1	G 67.4 (0.20) N 251.4 (0.61) Iso
Poly-DNA-OC3	Cr 113.8 (5.37) N 246.5 (0.61) Iso
Poly-DNA-OC6	Cr 140.0 (5.42) SmC 178.1 (0.47) N 231.2 (0.62) Iso

[a] Transition temperatures were determined upon cooling process.

Mesomorphic properties

The phase sequential properties upon cooling, of both the monomeric compounds (mono-DNA-OC*m*) and polymers (poly-DNA-OC*m*) are listed in Table 2. All monomers showed enantiotropic crystal (Cr)–N and N–isotropic (Iso) phase transitions upon heating and cooling. Interestingly, all compounds showed a wide N temperature range over 50 °C, implying that the DNA mesogenic unit had sufficient potential as a nematogenic monomer unit. On the other hand, the mesomorphic properties of the polymers seemed to be much more complicated than those of the monomers. First, the appearance of an additional smectic C (SmC) phase was observed for poly-DNA-OC6 between the Cr and N phases, which might be caused by the extension of the alkoxy length in the pendant side-chain. Upon polymerisation, it was clear that the isotropisation temperatures (T_i) of the polymers were higher than those of the monomers, which was the result of both the degree of polymerisation and carbon number of the terminal chain (*m*). However, the melting temperature remained near 100 °C, except for the $m = 6$ homologue. First, the most noticeable effect of polymerisation was an expansion of the N phase temperature range, which was basically derived from the elevation of T_i; consequently, a wide N temperature range over 100 °C was realised, which was more than double that of the monomers. Thus, poly-DNA-OC*m* is definitely a promising material with high processability apart from its outstanding optical performance. Second, it was clearly observed that poly-DNA-OC1 showed a glass transition temperature (T_g) at 67 °C, which would provide a highly oriented N glassy film state at ambient temperature.

Optical properties

Measurement of Δn was performed for a homogeneously aligned N LC kept in a thin cell with rubbed polyimide.[9] Because the viscosities of the polymers were higher than those of the monomers, the polymers could hardly be loaded by capillary force. Thus, it was sandwiched between a pair of glass plates after heating to over T_i (the cell gap (d) was controlled between 4 and 6 μm using film spacers). The transmittance of light under cross-polarisation conditions was then observed as a function of wavelength, λ, by a microscope spectroscopic method. Here, the rubbing direction, *i.e.*, a N director, was set

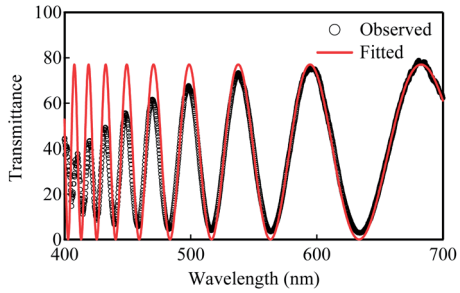

Fig. 1 Transmittance spectra observed for a glassy film of poly-DNA-OC1 at 25 °C (black open circle) and the fitted value (red solid line) by determination of Cauchy's coefficients. As can be seen, the fitted curve is in good agreement with the observed.

with an angle of 45° to the polarisers. Typical transmittance data obtained from poly-DNA-OC1 are shown in Fig. 1. As can be seen in Fig. 1, the transmitted light intensity, I, was fitted well by eqn (1) and Cauchy's eqn (2), leading to the determination of coefficients a, b and c. Here, A is constant.

$$\frac{I}{I_0} = A\sin^2\left(\frac{\pi d\Delta n(\lambda)}{\lambda}\right) \quad (1)$$

$$\Delta n(\lambda) = a + \frac{b}{\lambda^2} + \frac{c}{\lambda^4} \quad (2)$$

Fig. 2 shows the wavelength dispersions of Δn determined for poly-DNA-OCm ($m = 1$, 3 and 6). Firstly, for a comparison within the nematic phase, the Δn values were plotted against the same reduced temperature, $T/T_i = 0.9$ as shown in Fig. 2 (a). Here, the Δn values showed an increase with decreasing terminal chain length, m, from 6 to 1 even though the absolute temperatures of measurements also increase by decreasing m. This decrease resulted from a dilution effect in which an increase in the number of carbon atoms in the alkoxy tail contributed less to the molecular polarisability because its contribution to the optical anisotropy of molecules per unit volume was less effective than that of a conjugated moiety.[16,17] Secondly, in order to confirm the best optical performance for each material, Δn values were also plotted with their highest values, which were collected at 110 °C (N phase) for poly-DNA-OC3, 160 °C (SmC phase) for poly-DNA-OC6 and at room temperature (N glassy film) for poly-DNA-OC1. Interestingly, in this case, not only a dilution effect of the terminal chain length but also a vitrification effect could be responsible for the notable increase in Δn observed for a nematic glassy film of poly-DNA-OC1. This will be discussed in detail below. The highest among the measured values was 0.36 at 550 nm for poly-DNA-OC1, which showed significant improvement by 20% from the value of 0.3 at 550 nm previously reported for the DPDA-based side-chain LC polymer.[10]

To visualise the temperature dependence of birefringence and compare it among the homologues, the Δn values collected at 550 nm were plotted against the temperature as shown in Fig. 3. In the higher temperature region near the isotropic–N transition temperature (T_i), the polymers exhibited relatively low birefringence, whereas birefringence gradually increased with decreasing temperature. This result could be explained by the temperature dependence of the order parameter (S) of the N director, which is well described by Haller's approximation given in the following equations.[18]

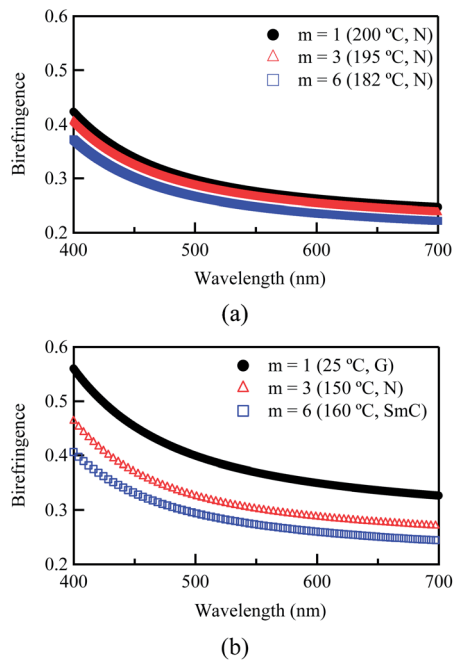

Fig. 2 Wavelength dispersions of birefringence for poly-DNA-OCm compared with (a) the same reduced temperature ($T/T_i = 0.9$) in the nematic phase and (b) their highest values at the nematic glass state, nematic phase and smectic C phase for $m = 1$, 3 and 6, respectively.

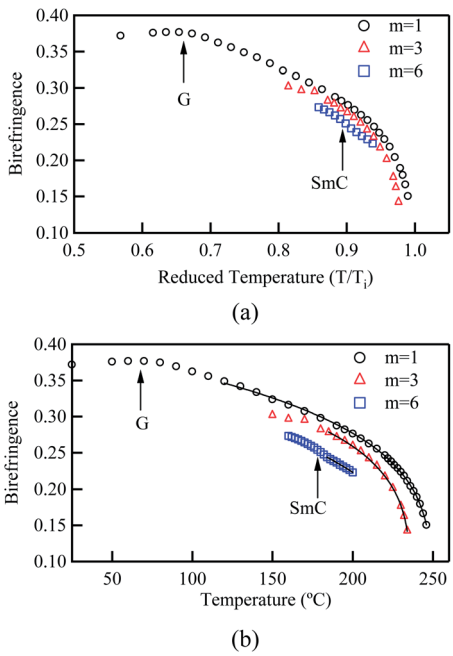

Fig. 3 Temperature dependence of birefringences obtained for poly-DNA-OCm. (a) Plotted against reduced temperature. (b) Plotted against temperature and fitted by eqn (3) and (4). For $m = 3$ and 6 compounds, the fitting was performed within the nematic phase region. The arrows indicate glass transition and N to SmC transition points.

Table 3 Determined values of Δn_0 and β by Haller's approximation

m	Δn_0	β	T_i
1	0.479	0.233	249.6
3	0.455	0.213	236.2
6	0.417	0.236	235.3

$$\Delta n = \Delta n_0 S \quad (3)$$

$$S = \left(1 - \frac{T}{T_i}\right)^{\beta} \quad (4)$$

here, Δn_0 is the extrapolation value that is, the birefringence expected for a perfectly oriented N LC and β is the material constant characteristic of the N LC. This equation fits well as shown in Fig. 3 and the determined values of Δn_0 and β are listed in Table 3. Among the polymers, poly-DNA-OC1 showed a noteworthy trend. Near the T_g, Δn reached the highest value, deviating from the expected fitting value of 120 °C, which could be the result of vitrification of the N LC. In other words, the highest optical performance of poly-DNA-OC1 films could be achieved in the solid film. The order parameter at room temperature calculated by eqn (3) was approximately 0.76 and when the order parameter was 1, which is attained by coupling of the elongation, the film held a Δn value of 0.479 at 550 nm. This is definitely a high value and is a promising characteristic of these materials that can find various usages in fabrication of optical devices.

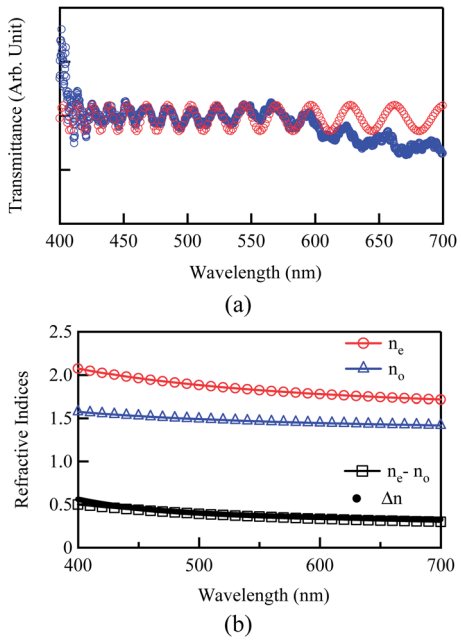

Fig. 4 (a) A typical example of the transmittance spectra (blue open circle) observed perpendicular to the nematic director for poly-DNA-OC1 at room temperature. Curve fitting (red open circle) was also performed in order to obtain the ordinary refractive index. (b) Wavelength dispersion of extraordinary (n_e) and ordinary (n_o) refractive indices and $n_e - n_o$ measured for the poly-DNA-OC1 film at room temperature. Δn value presented in Fig. 2 is also plotted simultaneously.

For a more detailed analysis of the optical performance, we measured an extraordinary refractive index, n_e and an ordinary refractive index, n_o using a multiple-beam interference (MBI) method.[19] Measurement of transmitted intensity *via* MBI was performed using two geometries in which the linearly polarised incident light was set either parallel or perpendicular to the direction of the N director, ñ. Here, the extraordinary and ordinary refractive indices were defined with optical geometries that allowed the transmitted light intensity to be observed, such that the plane of the linearly polarised incident rays was parallel or perpendicular to the molecular long axis.[17]

A representative transmittance spectrum is presented in Fig. 4(a), as observed for the poly-DNA-OC1 film with polarised incident light perpendicular to the molecular orientation that is, measuring ordinary refractive index. The spectra were then curve-fitted using eqn (5) to determine the coefficients a and b.

For normal incidence, the transmittance intensity can be expressed as:

$$\frac{I_t}{I_i} = \frac{1}{1 + A' \sin^2\left(\frac{2\pi}{\lambda} nd\right)} \approx \left[1 - A' \sin^2\left(\frac{2\pi}{\lambda} nd\right)\right] \quad (5)$$

$$A' = \left[\frac{n_1^2(\lambda) - n_2^2(\lambda)}{2n_1(\lambda)n_2(\lambda)}\right]^2$$

$$n(\lambda) = a + \frac{b}{\lambda^2} \quad (6)$$

where n_1 and n_2 are the refractive indices of the glass and the LC polymer media, respectively. Here, the wavelength dependence of A' is ignored because the final value of A' can be considered small. By utilising Cauchy's eqn (6) with the determined coefficients a and b, we obtained the values and wavelength dispersions of n_e and n_o as well as the difference between n_e and n_o as presented in Fig. 4(b). First, the high Δn property of DNA-OC1 can be attributed to the high extraordinary refractive index of 1.82 at 550 nm, whereas the ordinary refractive index was 1.46. Second, both birefringence values of $n_e - n_o$ and Δn simultaneously plotted in Fig. 4(b) show good agreement with each other, which implies that our measurement of n_e and n_o was sufficiently reliable.

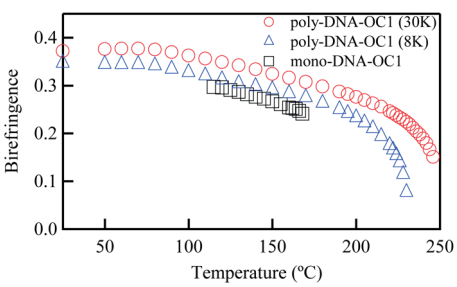

Fig. 5 Temperature dependence of birefringences obtained for mono-DNA-OC1 and poly-DNA-OC1 with different molecular weights of 30 000 and 8000. Not only polymerisation but also the degree of polymerisation affects the absolute value of birefringence.

Finally, the optical properties of the monomer and polymers were compared. Fig. 5 shows the typical temperature dependence of birefringence observed for mono-DNA-OC1, poly-DNA-OC1 (8k) with M_w = 8000 and poly-DNA-OC1 (30k) with M_w = 30 000. It is apparent that the Δn value increased by polymerisation as demonstrated by a comparison between mono-DNA-OC1 and poly-DNA-OC1. Further, an increase in birefringence was obvious with increasing molecular weight from 8000 to 30 000. This feature is striking from the view point of molecular polarisability per unit volume, because the polymer main chain backbone would be in a perpendicular direction to the side chain mesogenic moiety and then the polymerisation seemed to have less effect on the Δn value. One possible explanation for the increase in the Δn value by polymerisation and with an increase in M_w might be an increase in the order parameter upon polymerisation. To compare the order parameters of poly-DNA-OC1 (30k) and mono-DNA-OC1, $\Delta n/\Delta n_0$ values (at 550 nm) were calculated at room temperature and 115 °C (N phase) for the poly-DNA-OC1 glassy film and mono-DNA-OC1, respectively. As already presented in Fig. 5, the former gave a $\Delta n/\Delta n_0$ = 0.76 whereas the latter gave a $\Delta n/\Delta n_0$ = 0.70, which is apparently smaller for the monomer than the polymer unit. Then, once again we have confirmed their order parameters *via* X-ray measurements for oriented samples using a magnetic field. Fig. 6(a) and (b) show typical oriented wide-angle X-ray diffraction (WAXD) patterns obtained for the poly-DNA-OC1 film and mono-DNA-OC1 at room temperature and N phase (140 °C), respectively. As can be seen from the diffraction patterns, the outer broad diffractions at $q\ (= 2\pi/d) = 2\pi/4.4$ Å^{-1} were located on the equatorial line, indicating the uniaxial alignment of mesogenic units, *i.e.*, the side chains were successfully oriented parallel to the magnetic field. However, it was obvious that the degree of orientation was higher in the polymer (Fig. 6(a)) than in the monomer (Fig. 6(b)) as clearly shown in Fig. 6(c), which shows the beta scan profile of the outer diffractions observed in Fig. 6(a) and (b). The order parameter, S_X (here, we adopted a subscripted '*x*' to distinguish it from the order parameter, S, calculated from the birefringence observations) was induced with the distribution of azimuthal angle (β) and the corresponding intensity, $I(\beta)$, into the conventional equation:[20]

$$S_X = \frac{\left(3\langle\cos^2\beta\rangle - 1\right)}{2} \tag{7}$$

where the average cosine square, $\langle\cos^2\beta\rangle$, was obtained from the following equation:

$$\langle\cos^2\beta\rangle = \frac{\int_0^{\pi/2} I(\beta)\cos^2\beta|\sin\beta|\mathrm{d}\beta}{\int_0^{\pi/2} I(\beta)|\sin\beta|\mathrm{d}\beta} \tag{8}$$

The calculated S_X values were 0.79 for the poly-DNA-OC1 film at room temperature and 0.57 for mono-DNA-OC1 at 140 °C, which were consistent with the order parameter, *S*, observed from the birefringence measurements. Here, the S_X for mono-DNA-OC1 was 0.57, which is smaller than the $\Delta n/\Delta n_0$ = 0.70 at 115 °C. However, this difference seems to be the result of the measuring temperature as the X-ray measurement was performed at a slightly higher temperature of 140 °C. At 140 °C, a $\Delta n/\Delta n_0$ of 0.66 was calculated. Thus, it could be concluded that the order parameters derived from the WAXD measurements also showed the same result that the polymer could obtain a higher orientation in the glassy film than the monomer's degree of orientation in the N phase.

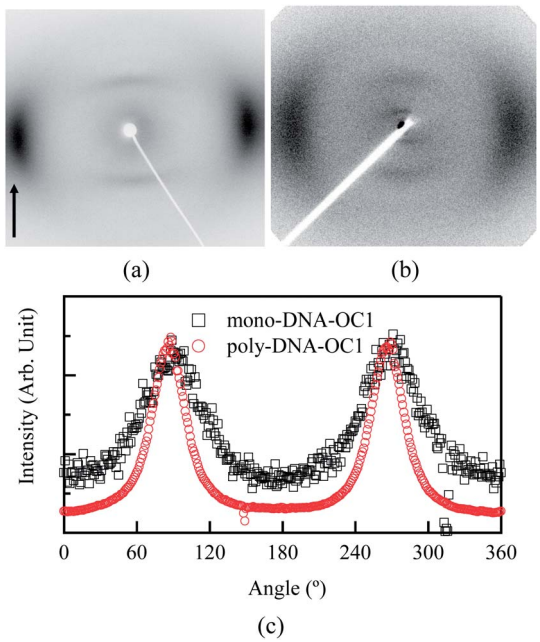

Fig. 6 Oriented patterns of WAXD measurements for (a) poly-DNA-OC1 film at room temperature and (b) mono-DNA-OC1 at 140 °C. (c) Azimuthal scans of outer broad reflections shown in (a) and (b) located on the equatorial line at $2\pi/4.4$ Å^{-1}.

Here, it can be assumed that polymerisation can affect the order parameter in a way that suppresses the individual fluctuation of side chain deviation from the average direction of mesogens, n-director, by tying up one of the terminal chains into the rigid polymer backbone. Thus, the length of the spacer (here, the number of carbon atoms is six) is thought to have an important role that can also affect the optical properties combined with the factor of molecular weight. Consequently, effects of both polymerisation and vitrification seem to be attributable to the current observation of high birefringence in poly-DNA-OC1 with higher molecular weight.

Conclusions

By radical polymerisation, we synthesised highly birefringent side-chain LC polymers, poly-DNA-OC*m*, which were composed of PM with a DNA mesogenic moiety in the side chain. Furthermore, we evaluated the optical performance of these polymers, including birefringence and extraordinary and ordinary refractive indices. Notably, we also succeeded in obtaining a N glassy film of poly-DNA-OC1 with excellent optical properties at room temperature. Owing to not only high optical performance of the DNA mesogenic unit, but also to a higher order parameter effect that is derived from the vitrification at

the ambient temperature region, the poly-DNA-OC1 film exhibits a significantly high birefringence of 0.36, $n_e = 1.82$, and $n_o = 1.46$ at 550 nm, which exceed those of the monomer. We believe this optical performance can be attributed to both the polymerisation and vitrification effects of the poly-DNA-OC1 glassy film resulting from the higher order parameter of polymeric compounds. This study provides a potential solution involving a LC polymer that is transparent and can be used at ambient temperature with significantly high optical ability for future development of optical films.

Experimental section

Measurement of optical and thermodynamic properties and X-ray investigation

The phase determinations were carefully made by using POM observations, DSC measurements and WAXD investigations.[21]

Optical textures were observed under a crossed polariser using a Nikon LV100 Pol polarising optical microscopy system. Transition temperatures and the corresponding enthalpies were determined by differential scanning calorimetry using a Perkin-Elmer Pyris 1 calorimeter. The Δn measurement was performed by a microscopic spectroscopy method using a Nikon LV100 Pol optical microscope equipped with a USB4000 (Ocean Photonics) spectrometer. X-ray investigations were carried out with samples kept in glass capillary tubes (1.5 mm diameter) for oriented patterns under either a magnetic field or superconductive magnetic field. WAXD measurements were performed using both a Rigaku RINT-2500 X-ray generator equipped with a flat plate-type imaging plate and a Bruker D8 DISCOVER X-ray diffractometer equipped with a Vantec-500 detector using Cu–Kα radiation.

Acknowledgements

This study was supported by the Strategic Promotion of Innovative Research and Development from the Japan Science and Technology Agency, JST.

Notes and references

1 (*a*) S.-T. Wu, *Mol. Cryst. Liq. Cryst.*, 2004, **411**, 93; (*b*) K. Okano, A. Shishido and T. Ikeda, *Macromolecules*, 2006, **39**, 145.

2 (*a*) R. Ozaki, T. Matsui, M. Ozaki and K. Yoshino, *Appl. Phys. Lett.*, 2003, **82**, 3593; (*b*) J. Hwang, M. H. Song, B. Park, S. Nishimura, T. Toyooka, J. W. Wu, Y. Takanishi, K. Ishikawa and H. Takezoe, *Nat. Mater.*, 2005, **4**, 383; (*c*) M. Uchimura, Y. Watanabe, F. Araoka, J. Watanabe, H. Takezoe and G. Konishi, *Adv. Mater.*, 2010, **22**, 4473; (*d*) Y. Watanabe, M. Uchimura, F. Araoka, J. Watanabe, H. Takezoe and G. Konishi, *Appl. Phys. Express*, 2009, **2**, 102501.

3 (*a*) M. O'Neill and S. M. Kelly, *Adv. Mater.*, 2003, **15**, 1135; (*b*) Y. Matsuura, Y. Nam, M. Kinoshita and T. Ikeda, *Mol. Cryst. Liq. Cryst.*, 2009, **513**, 153.

4 (*a*) T. R. Wolinski, A. Szymanska, T. Nasilowski, M. A. Karpierz, A. Kujawski and R. Dabrowski, *Mol. Cryst. Liq. Cryst.*, 1998, **321**, 557; (*b*) S. Agnieszka and R. W. Tomasz, *Mol. Cryst. Liq. Cryst.*, 2002, **375**, 723.

5 (*a*) T. Yamamoto, M. Hasegawa, A. Kanazawa, T. Shiono and T. Ileda, *J. Mater. Chem.*, 2000, **10**, 337; (*b*) T. Ikeda, *J. Mater. Chem.*, 2003, **13**, 2037.

6 (*a*) Q. Song, S. Gauza, H. Xianyu, S.-T. Wu, Y.-M. Liao, C.-Y. Chang and C.-S. Hsu, *Liq. Cryst.*, 2010, **37**, 139; (*b*) M. Hird, K. J. Toyne, J. W. Goodby, G. W. Gray, V. Minter, R. P. Tuffin and D. G. McDonnell, *J. Mater. Chem.*, 2004, **14**, 1731.

7 (*a*) C. Sekine, K. Fujisawa, K. Iwakura and M. Minai, *Mol. Cryst. Liq. Cryst. Sci. Technol., Sect. A*, 2001, **364**, 711; (*b*) C. Sekine, K. Iwakura, N. Konya, M. Minai and K. Fujisawa, *Liq. Cryst.*, 2001, **28**, 1375.

8 (*a*) B. Grant, *Mol. Cryst. Liq. Cryst.*, 1978, **48**, 175; (*b*) B. Grant, N. J. Cleak and R. J. Cox, *Mol. Cryst. Liq. Cryst.*, 1979, **51**, 209; (*c*) S.-T. Wu and L. R. Dalton, *J. Appl. Phys.*, 1989, **65**, 4372; (*d*) S.-T. Wu, H. B. Meng and L. R. Dalton, *J. Appl. Phys.*, 1991, **70**, 3013.

9 (*a*) Y. Arakawa, S. Nakajima, R. Ishige, M. Uchimura, S. kang, G. Konishi and J. Watanabe, *J. Mater. Chem.*, 2012, **22**, 8394; (*b*) M. Uchimura, S. Kang, R. Ishige, J. Watanabe and G. Konishi, *Chem. Lett.*, 2010, 513; (*c*) Y. Arakawa, S. Nakajima, S. Kang, M. Shigeta, G. Konishi and J. Watanabe, *Liq. Cryst.*, 2012, **9**, 1063.

10 Y. Arakawa, S. Nakajima, S. Kang, M. Shigeta, G. Konishi and J. Watanabe, *J. Mater. Chem.*, 2012, **22**, 14346.

11 E. Negishi, M. Hata and C. Xu, *Org. Lett.*, 2000, **2**, 3687.

12 T. Katoh, T. Akagi, C. Noguchi, T. Kajimoto, M. Node, R. Tanaka, M. Nishizawa, H. Ohtsu, N. Suzuki and K. Saito, *Bioorg. Med. Chem.*, 2007, **15**, 2736.

13 (*a*) J. S. Hwang and T. Ogawa, *Polym. Bull.*, 1990, **23**, 239; (*b*) G. Burillo, T. Ogawa and J. S. Hwang, *J. Polym. Sci., Part A: Polym. Chem.*, 1992, **30**, 2159; (*c*) G. Canizal, G. Burillo, E. Munoz, R. Gleason and T. Ogawa, *J. Polym. Sci., Part A: Polym. Chem.*, 1994, **32**, 3147.

14 A. S. Kende and C. A. Smith, *J. Org. Chem.*, 1988, **53**, 2655.

15 See ESI: Synthesis procedures and NMR analysis data.†

16 G. Pelzl and H. Sackmann, *Symp. Faraday Soc.*, 1971, **5**, 68.

17 S. Kang, S. Nakajima, Y. Arakawa, G. Konishi and J. Watanabe, *J. Mater. Chem. C*, 2013, **1**, 4222.

18 I. Haller, *Prog. Solid State Chem.*, 1975, **10**, 103.

19 R. Chang, *Mol. Cryst. Liq. Cryst.*, 1974, **28**, 1.

20 L. E. Alexander, *X-ray diffraction methods in polymer science*, John Wiley & Sons, Inc., New York, 1969.

21 See ESI: POM micrographs of nematic and smectic phases are shown in Fig. S1; a WAXD profile obtained in smectic C phase for poly-DNA-OC6 is shown in Fig. S2.†

